The Effect of Phase and Amplitude Imbalance on the Performance of Offset Quadrature Phase-Shift-Keyed (OQPSK) Communication Systems

H. Tsou[1]

The balanced modulator, which comprises two amplitude-modulation modules, is widely used in phase-modulated communication systems. In practice, the balance between these amplitude-modulation modules is difficult to maintain, and the amplitude and phase imbalances can cause distortion in the signal constellation and introduce undesired interfering tone signal components when such an imperfect modulator is used to modulate the data directly onto the RF carrier. The rendered imperfection inevitably degrades the receiver performance and, in a quadrature phase-shift-keyed (QPSK) system, causes cross talk between the in-phase and quadrature-phase channels. This article summarizes an analysis of the impact of these modulator imbalances on an offset QPSK (OQPSK) communication system in which an OQPSK signal is coherently demodulated by using a carrier reference extracted from a modified QPSK carrier tracking loop. Both carrier-suppression level and bit-error performance are analyzed in this article. The results show that the current Consultative Committee for Space Data Systems (CCSDS) recommendations of 2-deg maximum permissible phase imbalance and 0.2-dB amplitude imbalance are sufficient to provide a 25-dB or more carrier suppression and a system degradation of 1 dB or less at the bit-error probability of 10^{-4} when the OQPSK system is operated in a reasonable loop SNR region.

I. Introduction

The balanced modulator [1], which comprises two amplitude-modulation (AM) modules, is widely used in phase-modulated communication systems. However, in practice, the balance between these AM modules is difficult to maintain and, when an imperfectly balanced modulator is used in missions where the carrier is directly modulated by data without using a subcarrier, the amplitude and phase imbalances not only cause distortion in the signal constellation but also introduce an interfering tone signal component at the carrier frequency. The imperfection rendered from the modulator imbalances inevitably degrades the receiver performance and, for a quadrature phase-shift-keyed (QPSK) system in particular, can cause cross talk between the in-phase (I) and quadrature-phase (Q) channels. For example, the spurious spectral line at the carrier frequency is detrimental to the carrier-tracking performance by forcing the steady-state

[1] Communications Systems and Research Section.

lock point of the carrier tracking loop away from its correct location. The presence of such an unwanted spectral line also raises the concern of exceeding the power flux density limit. Moreover, the combined effect of the imperfect channel separation from its ideal 90-deg angle in a QPSK system and the inaccurate phase reference caused by the imperfect carrier tracking degrades the bit-error performance.

This article summarizes a study of the impact of these modulator imbalances on a variant of the QPSK system, referred to as the offset QPSK (OQPSK). The model of modulator imbalances used in this study is adopted from [2] except that the Q-channel data stream is delayed by a half-symbol to achieve an OQPSK modulation and the amplitude imbalance between the I-channel and the Q-channel is added to be an additional independent parameter.[2] The carrier reference used for coherent OQPSK demodulation is derived from a modified IQ(I^2–Q^2)-type QPSK carrier tracking loop, in which a half-symbol delay is added to its in-phase arm so that the symbols on both arms are aligned.

In Section II of this article, the model of modulator imbalances on a typical OQPSK signal, of which the in-phase and quadrature-phase channels are intended to have the same bit rate and equal power, is provided. The effect of modulator imbalances on the carrier-suppression level and steady-state lock point of the OQPSK carrier tracking are derived in Sections III and IV. The averaged and individual bit-error performance for the combinations of amplitude and phase imbalances within the maximum permissible imbalance figures currently recommended by the Consultative Committee for Space Data Systems (CCSDS) [3] are evaluated in Section V, followed by a conclusion in Section VI presenting the worst-case performance expected with the recommended maximum permissible modulator imbalances.

II. Modulator Imbalances

The block diagram of an OQPSK modulator implemented by using two balanced modulators, each consisting of two AM modules, is shown in Fig. 1. In each channel, the binary, equally probable data in nonreturn-to-zero (NRZ) format are fed into these two AM modules, one of them receiving the data stream with inverted polarity. For perfectly balanced AM modules, the AM signals subtract to form a binary phase-shift-keyed signal with unmodulated carrier completely suppressed. However, with the presence of modulator imbalances, the I-channel and Q-channel signals can be modeled, respectively, as

$$S_{01}(t) = \left(\frac{\sqrt{P}}{2}\right) m_1(t)\left[\cos(\omega_c t + \theta_1) + \Gamma_1 \cos(\omega_c t + \theta_1 + \Delta\theta_1)\right]$$

$$+ \left(\frac{\sqrt{P}}{2}\right)\left[\cos(\omega_c t + \theta_1) - \Gamma_1 \cos(\omega_c t + \theta_1 + \Delta\theta_1)\right] \tag{1}$$

and

$$S_{02} = \Gamma\left(\frac{\sqrt{P}}{2}\right) m_2\left(t - \frac{T_s}{2}\right)\left[\sin(\omega_c t + \theta_2) + \Gamma_2 \sin(\omega_c t + \theta_2 + \Delta\theta_2)\right]$$

$$+ \Gamma\left(\frac{\sqrt{P}}{2}\right)\left[\sin(\omega_c t + \theta_2) - \Gamma_2 \sin(\omega_c t + \theta_2 + \Delta\theta_2)\right] \tag{2}$$

where

[2] The interchannel amplitude imbalance does exist in [2], but in an implicit way such that it can be determined through the combination of amplitude and phase imbalances in individual channels.

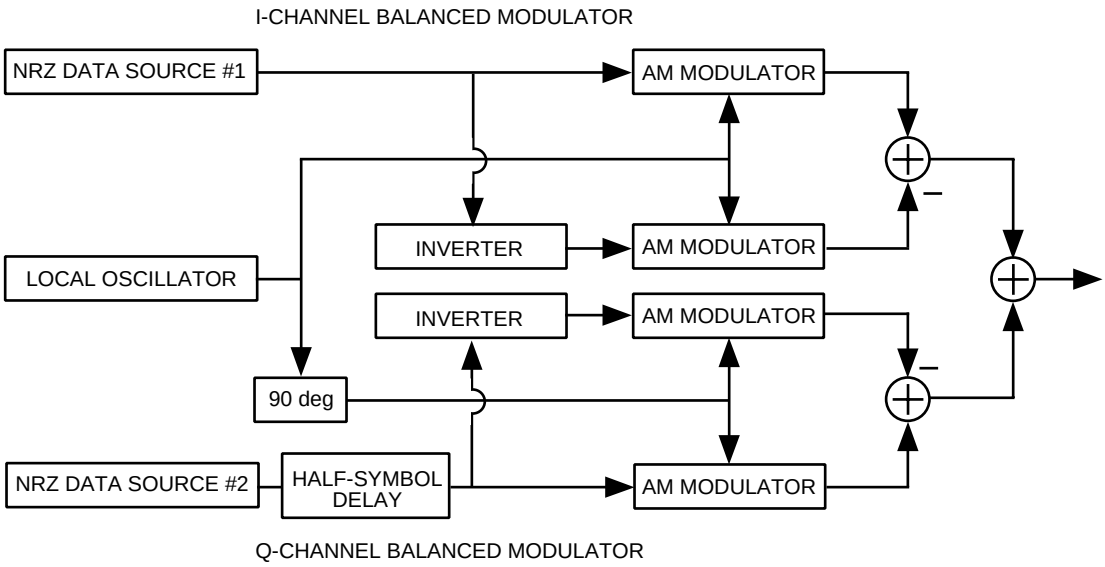

Fig. 1. The OQPSK modulator.

$P =$ the total power

$T_s =$ the symbol duration

$m_1(t), m_2(t) =$ equally probable, binary NRZ data streams for the I-channel and Q-channel, respectively

$\Gamma =$ the relative amplitude imbalance (assumed to be less than 1) between the I-channel and Q-channel balanced modulators

$\theta_1, \theta_2 =$ the local oscillator phases of the I-channel and Q-channel balanced modulators, respectively

$\Gamma_1, \Gamma_2 =$ the relative amplitude imbalances in the I-channel and Q-channel balanced modulators, respectively

$\Delta\theta_1, \Delta\theta_2 =$ the phase errors caused by the unbalanced AM modulators in the I-channel and Q-channel balanced modulators, respectively.

The resulting OQPSK signal, $S_0(t) = S_{01}(t) + S_{02}(t)$, is the combination of the I-channel and Q-channel signals. It is obvious that, in both Eqs. (1) and (2), the first terms are the desired modulated signal components and the second terms are the interfering carrier components, all affected by the modulator imbalances. Figure 2 shows the phasor representation of the resulting OQPSK signal, in which the interchannel phase error, denoted as $\Delta\theta = \theta_1 - \theta_2$, is the phase deviation from the ideal 90-deg separation between the I-channel and the Q-channel. By assuming $\theta_2 = 0$, without loss of generality, the signal can be rewritten as

$$S_0(t) = \sqrt{P}\big[(\alpha_1 \cos\omega_c t + \delta_1 \sin\omega_c t) + m_1(t)(\beta_1 \cos\omega_c t - \gamma_1 \sin\omega_c t)\big]$$

$$+ \sqrt{P}\left[(\alpha_2 \sin\omega_c t - \gamma_2 \cos\omega_c t) + m_2\left(t - \frac{T_s}{2}\right)(\beta_2 \sin\omega_c t + \gamma_2 \cos\omega_c t)\right] \tag{3}$$

where

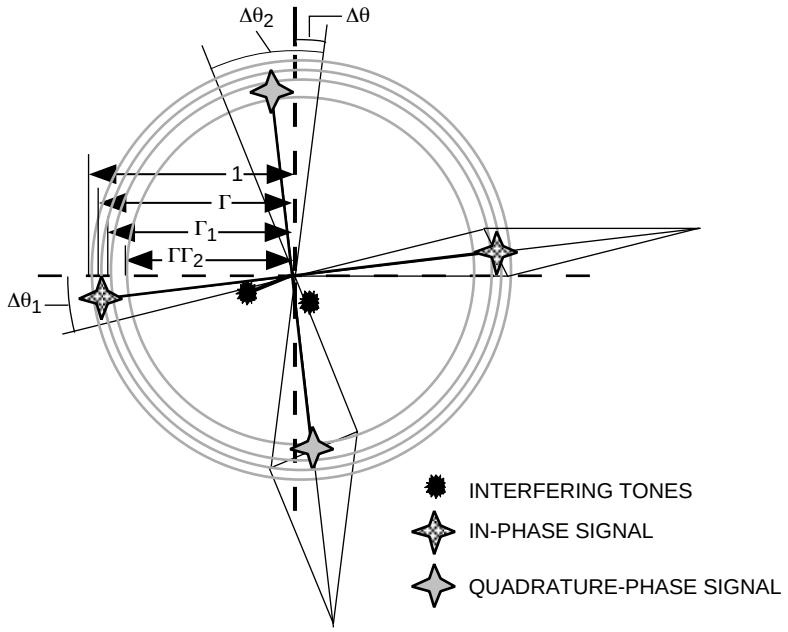

Fig. 2. Phasor diagram of the OQPSK signal.

$$\alpha_1 = \frac{(1 - \Gamma_1 \cos\Delta\theta_1)\cos\Delta\theta + \Gamma_1 \sin\Delta\theta_1 \sin\Delta\theta}{2}$$

$$\alpha_2 = \Gamma\left(\frac{1 - \Gamma_2 \cos\Delta\theta_2}{2}\right)$$

$$\beta_1 = \frac{(1 + \Gamma_1 \cos\Delta\theta_1)\cos\Delta\theta - \Gamma_1 \sin\Delta\theta_1 \sin\Delta\theta}{2}$$

$$\beta_2 = \Gamma\left(\frac{1 + \Gamma_2 \cos\Delta\theta_2}{2}\right)$$

$$\gamma_1 = \frac{(1 + \Gamma_1 \cos\Delta\theta_1)\sin\Delta\theta + \Gamma_1 \sin\Delta\theta_1 \cos\Delta\theta}{2}$$

$$\gamma_2 = \Gamma\left(\frac{\Gamma_2 \sin\Delta\theta_2}{2}\right)$$

$$\delta_1 = \frac{-(1 - \Gamma_1 \cos\Delta\theta_1)\sin\Delta\theta + \Gamma_1 \sin\Delta\theta_1 \cos\Delta\theta}{2}$$

or, equivalently, as

$$S_0(t) = \sqrt{P}\left[\alpha_1 + \beta_1 m_1(t) - \gamma_2\left(1 - m_2\left(t - \frac{T_s}{2}\right)\right)\right]\cos\omega_c t + \sqrt{P}\left[\alpha_2 + \beta_2 m_2\left(t - \frac{T_s}{2}\right) + \delta_1 - \gamma_1 m_1(t)\right]\sin\omega_c t \quad (4)$$

where the cross talk introduced by modulator imbalances is clearly identified. For the case of $\Delta\theta_1 = \Delta\theta_2 = \Delta\theta = 0$, the cross talk disappears from the modulated signal. However, the lack of cross talk in a modulated signal does not guarantee the absence of cross talk on the receiver side. Actually, cross talk may happen simply because of imperfect carrier tracking even though the orthogonality between the I-channel and the Q-channel is precisely maintained.

III. Carrier-Suppression Level

The spurious carrier component resulting from the modulator imbalances, described by Eq. (4), is found to be

$$\sqrt{P}\big[(\alpha_1 - \gamma_2)\cos\omega_c t + (\alpha_2 + \delta_1)\sin\omega_c t\big] \tag{5}$$

with an average power of

$$\left(\frac{P}{2}\right)\left[(\alpha_1 - \gamma_2)^2 + (\alpha_2 + \delta_1)^2\right] \triangleq \left(\frac{P}{2}\right)\eta \tag{6}$$

where η, typically expressed in dB, is referred to as the carrier-suppression level.

Table 1 provides the carrier-suppression levels calculated for various combinations of worst-case OQPSK modulator imbalances, which are recommended in [3] as 2 deg for phase imbalance and 0.2 dB for amplitude imbalance. The resulting carrier-suppression level actually varies in a range approximately from -25 to -42 dB.

Table 1. Carrier-suppression levels under various combinations of modulator imbalances (I/Q power ratio = 0 dB).

$\Delta\theta$, deg	Γ_1, dB	$\Delta\theta_1$, deg	Γ_2, dB	$\Delta\theta_2$, deg	Carrier suppression level, dB
0	0.0	0	0.0	0	$-\infty$
0	−0.2	2	−0.2	2	−27.9735
0	−0.2	2	0.0	2	−34.9961
0	0.0	2	−0.2	2	−27.2417
0	0.0	2	0.0	2	−32.1526
0	−0.2	2	−0.2	−2	−25.0668
0	−0.2	2	0.0	−2	−27.1952
0	0.0	2	−0.2	−2	−27.1952
0	0.0	2	0.0	−2	−32.0036
0	−0.2	−2	−0.2	2	−41.2402
0	−0.2	−2	0.0	2	−35.2840
0	0.0	−2	−0.2	2	−35.2840
0	0.0	−2	0.0	2	−32.3069
0	−0.2	−2	−0.2	−2	−27.9735

Table 1 cont'd.

$\Delta\theta$, deg	Γ_1, dB	$\Delta\theta_1$, deg	Γ_2, dB	$\Delta\theta_2$, deg	Carrier suppression level, dB
0	−0.2	−2	0.0	−2	−27.2417
0	0.0	−2	−0.2	−2	−34.9961
0	0.0	−2	0.0	−2	−32.1526
2	−0.2	2	−0.2	2	−28.1278
2	−0.2	2	0.0	2	−35.2840
2	0.0	2	−0.2	2	−27.2909
2	0.0	2	0.0	2	−32.3069
2	−0.2	2	−0.2	−2	−25.0917
2	−0.2	2	0.0	−2	−27.1515
2	0.0	2	−0.2	−2	−27.1515
2	0.0	2	0.0	−2	−31.8597
2	−0.2	−2	−0.2	2	−42.2767
2	−0.2	−2	0.0	2	−34.9961
2	0.0	−2	−0.2	2	−34.9961
2	0.0	−2	0.0	2	−32.1526
2	−0.2	−2	−0.2	−2	−28.1278
2	−0.2	−2	0.0	−2	−27.2909
2	0.0	−2	−0.2	−2	−35.2840
2	0.0	−2	0.0	−2	−32.3069
−2	−0.2	2	−0.2	2	−27.8245
−2	−0.2	2	0.0	2	−34.7138
−2	0.0	2	−0.2	2	−27.1952
−2	0.0	2	0.0	2	−32.0036
−2	−0.2	2	−0.2	−2	−25.0446
−2	−0.2	2	0.0	−2	−27.2417
−2	0.0	2	−0.2	−2	−27.2417
−2	0.0	2	0.0	−2	−32.1526
−2	−0.2	−2	−0.2	2	−40.3167
−2	−0.2	−2	0.0	2	−35.5769
−2	0.0	−2	−0.2	2	−35.5769
−2	0.0	−2	0.0	2	−32.4666
−2	−0.2	−2	−0.2	−2	−27.8245
−2	−0.2	−2	0.0	−2	−27.1952
−2	0.0	−2	−0.2	−2	−34.7138
−2	0.0	−2	0.0	−2	−32.0036

IV. Steady-State Lock Point of the Carrier Tracking Loop

To track the suppressed carrier of an OQPSK signal, the received signal entering the generalized Costas loop, shown in Fig. 3, first is mixed with the I-arm and Q-arm reference signals, i.e., $\sqrt{2}\cos(\omega_c t - \phi)$ and $\sqrt{2}\sin(\omega_c t - \phi)$, with ϕ being the error in the estimated carrier phase. Each of the resulting signals then is passed through an integrate-and-dump filter, which is assumed to be driven by a perfectly synchronized symbol timing clock, rendering

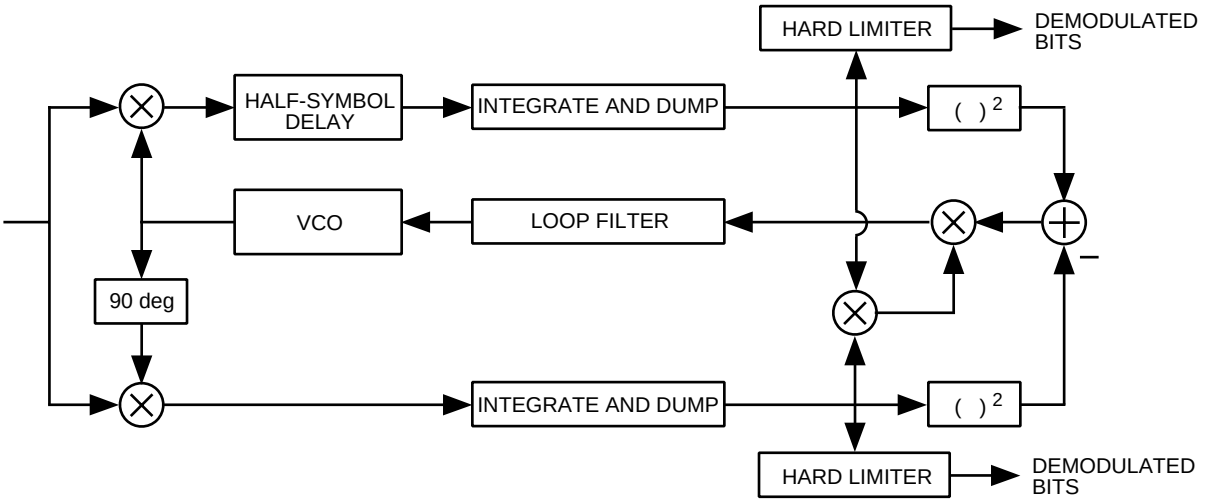

Fig. 3. The generalized Costas loop for OQPSK signals.

$$V_1 = \sqrt{\frac{P}{2}}T_s$$

$$\times \left[\left(\alpha_1 + \beta_1 a_0 - \gamma_2\left(1 - \frac{b_0 + b_{-1}}{2}\right)\right)\cos\phi + \left(\alpha_2 + \beta_2\left(\frac{b_0 + b_{-1}}{2}\right) + \delta_1 - \gamma_1 a_0\right)\sin\phi\right]$$

$$V_2 = \sqrt{\frac{P}{2}}T_s$$

$$\times \left[-\left(\alpha_1 + \beta_1\left(\frac{a_0 + a_{-1}}{2}\right) - \gamma_2(1 - b_{-1})\right)\sin\phi + \left(\alpha_2 + \beta_2 b_{-1} + \delta_1 - \gamma_1\left(\frac{a_0 + a_{-1}}{2}\right)\right) + \cos\phi\right] \tag{7}$$

where a_0, a_{-1}, b_0, and b_{-1} are the data bits from the in-phase and quadrature-phase data streams, each taking on values ± 1 with equal probability. The loop error signal, denoted as z_0, then is formed from

$$z_0 = V_1 V_2 \left(V_1^2 - V_2^2\right) \tag{8}$$

Carrying out the average over a_0, a_{-1}, b_0, and b_{-1} and equating to zero the averaged error signal, denoted as $\overline{z_0}$, one can solve for the steady-state lock point, denoted as ϕ_0, of this loop. The closed-form solution of such a generalized Costas loop is very involved, including all six arguments (i.e., $\Gamma, \Gamma_1, \Gamma_2, \Delta\theta_1, \Delta\theta_2$, and $\Delta\theta$), and, in general, can be solved only numerically. However, a quick check for the special case of no existing modulator imbalances agrees with the result given in [4].

V. Bit-Error Performance

The error performance is determined by the average bit-error probability associated with the demodulated data streams. It can be calculated by first finding the conditional (on the carrier-phase error) bit-error probability, $P_b(\phi)$, for a given carrier-phase error, ϕ, and then taking the average over the probability density function of the phase error, denoted as $p(\phi)$, as characterized by the carrier tracking loop.

For OQPSK signals, making hard decisions on V_1 and V_2 in Eq. (7) produces the decisions on the bits a_0 and b_0, respectively. It can be shown that, when the transmitted signal is corrupted by additive white Gaussian noise with two-sided power spectral density $N_0/2$ W/Hz, the conditional bit-error probabilities associated with these decisions are given by

$$\begin{aligned}
P_{b,1}(\phi) = {} & \frac{1}{16}\ \mathrm{erfc}\left(\sqrt{\frac{E_b}{N_0}}\left[\cos(\phi+\Delta\theta)+\Gamma\sin\phi\right]\right) \\
& + \frac{1}{16}\ \mathrm{erfc}\left(\sqrt{\frac{E_b}{N_0}}\left[\cos(\phi+\Delta\theta)-\Gamma\Gamma_2\sin(\phi+\Delta\theta_2)\right]\right) \\
& + \frac{1}{16}\ \mathrm{erfc}\left(\sqrt{\frac{E_b}{N_0}}\left[\Gamma_1\cos(\phi+\Delta\theta_1+\Delta\theta)-\Gamma\sin\phi\right]\right) \\
& + \frac{1}{16}\ \mathrm{erfc}\left(\sqrt{\frac{E_b}{N_0}}\left[\Gamma_1\cos(\phi+\Delta\theta_1+\Delta\theta)+\Gamma\Gamma_2\sin(\phi+\Delta\theta_2)\right]\right) \\
& + \frac{1}{8}\ \mathrm{erfc}\left(\sqrt{\frac{E_b}{N_0}}\left[\cos(\phi+\Delta\theta)-\frac{\Gamma\Gamma_2}{2}\sin(\phi+\Delta\theta_2)+\frac{\Gamma}{2}\sin\phi\right]\right) \\
& + \frac{1}{8}\ \mathrm{erfc}\left(\sqrt{\frac{E_b}{N_0}}\left[\Gamma_1\cos(\phi+\Delta\theta_1+\Delta\theta)+\frac{\Gamma\Gamma_2}{2}\sin(\phi+\Delta\theta_2)-\frac{\Gamma}{2}\sin\phi\right]\right) \qquad (9a)
\end{aligned}$$

and

$$\begin{aligned}
P_{b,2}(\phi) = {} & \frac{1}{16}\ \mathrm{erfc}\left(\sqrt{\frac{E_b}{N_0}}\left[\Gamma\cos\phi-\sin(\phi+\Delta\theta)\right]\right) \\
& + \frac{1}{16}\ \mathrm{erfc}\left(\sqrt{\frac{E_b}{N_0}}\left[\Gamma\cos\phi+\Gamma_1\sin(\phi+\Delta\theta_1+\Delta\theta)\right]\right) \\
& + \frac{1}{16}\ \mathrm{erfc}\left(\sqrt{\frac{E_b}{N_0}}\left[\Gamma\Gamma_2\cos(\phi+\Delta\theta_2)+\sin(\phi+\Delta\theta)\right]\right) \\
& + \frac{1}{16}\ \mathrm{erfc}\left(\sqrt{\frac{E_b}{N_0}}\left[\Gamma\Gamma_2\cos(\phi+\Delta\theta_2)-\Gamma_1\sin(\phi+\Delta\theta_1+\Delta\theta)\right]\right) \\
& + \frac{1}{8}\ \mathrm{erfc}\left(\sqrt{\frac{E_b}{N_0}}\left[\Gamma\cos\phi+\frac{\Gamma_1}{2}\sin(\phi+\Delta\theta_1+\Delta\theta)+\frac{1}{2}\sin(\phi+\Delta\theta)\right]\right) \\
& + \frac{1}{8}\ \mathrm{erfc}\left(\sqrt{\frac{E_b}{N_0}}\left[\Gamma\Gamma_2\cos(\phi+\Delta\theta_2)-\frac{\Gamma_1}{2}\sin(\phi+\Delta\theta_1+\Delta\theta)+\frac{1}{2}\sin(\phi+\Delta\theta)\right]\right) \qquad (9b)
\end{aligned}$$

where $E_b = (P/2)T_s$ is the bit energy and $P_{b,1}(\phi)$ and $P_{b,2}(\phi)$ are associated with the in-phase and quadrature-phase channels, respectively. Note that the bit-error performances of these two channels are, in general, not identical with the presence of modulator imbalances. The average bit-error probability for OQPSK signals is the arithmetic average of the bit-error probabilities of the I-channel and the Q-channel, given that they both have the same power and bit rate.

By substituting ϕ_0 found for the generalized Costas loop into Eqs. (9a) and (9b), the average bit-error probability and the individual bit-error probabilities for both channels can be evaluated as a function of E_b/N_0 for the loop operating at infinite loop signal-to-noise ratio (SNR), i.e., the case of perfect carrier synchronization. However, for realistic scenarios with imperfect carrier tracking due to the loop being operated at a finite loop SNR, a Tikhonov distribution is assumed for the carrier tracking phase error centered at ϕ_0 such that the probability density function of ϕ is

$$p(\phi) = \frac{2\exp\big(\rho_{4\phi}\cos\big(4(\phi-\phi_0)\big)\big)}{\pi I_0(\rho_{4\phi})} \tag{10}$$

where $I_0(\cdot)$ is the modified Bessel function of order zero and

$$\rho_{4\phi} = \frac{1}{\sigma_{4\phi}^2} = \frac{1}{16\sigma_{\phi}^2} \triangleq \frac{1}{16} \times (\text{loop SNR}) \tag{11}$$

By further assuming that the 90-deg phase ambiguity can be perfectly resolved, the average bit-error probability can be evaluated as

$$P_{b,1} = \int_{\phi_0-(\pi/4)}^{\phi_0+(\pi/4)} P_{b,1}(\phi)p(\phi)d\phi \tag{12a}$$

and

$$P_{b,2} = \int_{\phi_0-(\pi/4)}^{\phi_0+(\pi/4)} P_{b,2}(\phi)p(\phi)d\phi \tag{12b}$$

where $P_{b,1}$ and $P_{b,2}$ are associated with the I-channel and the Q-channel, respectively, and $p(\phi)$ is given in Eq. (10).

To illustrate the worst-case scenario, the following performance comparisons are all based upon the assumption that the actual power in the Q-channel is 0.4-dB less than that in the I-channel or, equivalently, the amplitude imbalance $\Gamma = -0.2$ dB. Tables 2 and 3 list the average and individual bit-error probabilities at an E_b/N_0 of 4 dB and 10 dB, respectively, for the possible combinations within the range constrained by a 0.2-dB maximum amplitude imbalance, a 2-deg maximum phase imbalance, and a 2-deg maximum phase deviation from the ideal 90-deg separation between channels. It is interesting to observe that performance degradation exists in all of the cases evaluated here, even if the signal constellation is orthogonal and the steady-state lock point of the tracking loop is correctly located, e.g., those four cases labeled with both (1) and (2) in the remarks column of these tables. The cause of a small degradation in these four cases is from their interfering carrier components. Also, both highly unbalanced and balanced bit-error performances among those two channels can be identified for certain combinations from these tables, indicating how different these channels can be when the modulator imbalances exist.

Table 2. OQPSK bit-error performance under various combinations of modulator imbalances (I/Q power ratio = 0.4 dB, E_b/N_0 = 4 dB).

$\Delta\theta$, deg	Γ_1, dB	$\Delta\theta_1$, deg	Γ_2, dB	$\Delta\theta_2$, deg	$P_{b,avg}$ at $E_b/N_0 = 4$ dB	$P_{b,I}$ at $E_b/N_0 = 4$ dB	$P_{b,Q}$ at $E_b/N_0 = 4$ dB	ϕ_0, deg	Remarks
0	0.0	0	0.0	0	1.4329×10^{-2}	1.2501×10^{-2}	1.6157×10^{-2}	0.0000	Best case
0	−0.2	2	−0.2	2	1.6408×10^{-2}	1.4248×10^{-2}	1.8568×10^{-2}	−0.9790	
0	−0.2	2	0.0	2	1.5240×10^{-2}	1.4247×10^{-2}	1.6234×10^{-2}	−0.9892	
0	0.0	2	−0.2	2	1.5568×10^{-2}	1.2560×10^{-2}	1.8576×10^{-2}	−0.9797	(c)
0	0.0	2	0.0	2	1.4400×10^{-2}	1.2563×10^{-2}	1.6237×10^{-2}	−0.9976	(a), (b)
0	−0.2	2	−0.2	−2	1.6595×10^{-2}	1.4576×10^{-2}	1.8614×10^{-2}	0.0322	
0	−0.2	2	0.0	−2	1.5433×10^{-2}	1.4590×10^{-2}	1.6277×10^{-2}	0.0336	
0	0.0	2	−0.2	−2	1.5613×10^{-2}	1.2593×10^{-2}	1.8632×10^{-2}	0.0468	(c)
0	0.0	2	0.0	−2	1.4443×10^{-2}	1.2600×10^{-2}	1.6287×10^{-2}	0.0436	(b)
0	−0.2	−2	−0.2	2	1.6279×10^{-2}	1.4285×10^{-2}	1.8273×10^{-2}	−0.0454	
0	−0.2	−2	0.0	2	1.5280×10^{-2}	1.4286×10^{-2}	1.6273×10^{-2}	−0.0337	
0	0.0	−2	−0.2	2	1.5432×10^{-2}	1.2589×10^{-2}	1.8275×10^{-2}	−0.0564	
0	0.0	−2	0.0	2	1.4439×10^{-2}	1.2596×10^{-2}	1.6283×10^{-2}	−0.0484	(b)
0	−0.2	−2	−0.2	−2	1.6382×10^{-2}	1.4540×10^{-2}	1.8223×10^{-2}	0.9755	
0	−0.2	−2	0.0	−2	1.5390×10^{-2}	1.4546×10^{-2}	1.6234×10^{-2}	0.9917	
0	0.0	−2	−0.2	−2	1.5391×10^{-2}	1.2560×10^{-2}	1.8223×10^{-2}	0.9868	
0	0.0	−2	0.0	−2	1.4400×10^{-2}	1.2563×10^{-2}	1.6237×10^{-2}	1.0024	(a), (b)
2	−0.2	2	−0.2	2	1.6446×10^{-2}	1.4285×10^{-2}	1.8606×10^{-2}	−1.9352	
2	−0.2	2	0.0	2	1.5280×10^{-2}	1.4286×10^{-2}	1.6273×10^{-2}	−1.9663	
2	0.0	2	−0.2	2	1.5610×10^{-2}	1.2595×10^{-2}	1.8626×10^{-2}	−1.9125	(c)
2	0.0	2	0.0	2	1.4439×10^{-2}	1.2596×10^{-2}	1.6283×10^{-2}	−1.9516	(b)
2	−0.2	2	−0.2	−2	1.6724×10^{-2}	1.4687×10^{-2}	1.8761×10^{-2}	−0.9219	
2	−0.2	2	0.0	−2	1.5562×10^{-2}	1.4712×10^{-2}	1.6413×10^{-2}	−0.9412	
2	0.0	2	−0.2	−2	1.5745×10^{-2}	1.2694×10^{-2}	1.8796×10^{-2}	−0.8868	(c)
2	0.0	2	0.0	−2	1.4571×10^{-2}	1.2708×10^{-2}	1.6434×10^{-2}	−0.9109	(b)
2	−0.2	−2	−0.2	2	1.6236×10^{-2}	1.4248×10^{-2}	1.8223×10^{-2}	−0.9992	
2	−0.2	−2	0.0	2	1.5240×10^{-2}	1.4247×10^{-2}	1.6234×10^{-2}	−1.0108	
2	0.0	−2	−0.2	2	1.5391×10^{-2}	1.2560×10^{-2}	1.8223×10^{-2}	−0.9868	
2	0.0	−2	0.0	2	1.4400×10^{-2}	1.2563×10^{-2}	1.6237×10^{-2}	−1.0024	(a), (b)
2	−0.2	−2	−0.2	−2	1.6421×10^{-2}	1.4568×10^{-2}	1.8274×10^{-2}	0.0240	
2	−0.2	−2	0.0	−2	1.5432×10^{-2}	1.4583×10^{-2}	1.6281×10^{-2}	0.0169	
2	0.0	−2	−0.2	−2	1.5432×10^{-2}	1.2589×10^{-2}	1.8275×10^{-2}	0.0564	
2	0.0	−2	0.0	−2	1.4439×10^{-2}	1.2596×10^{-2}	1.6283×10^{-2}	0.0484	(b)
−2	−0.2	2	−0.2	2	1.6458×10^{-2}	1.4285×10^{-2}	1.8631×10^{-2}	−0.0228	
−2	−0.2	2	0.0	2	1.5286×10^{-2}	1.4286×10^{-2}	1.6286×10^{-2}	−0.0120	
−2	0.0	2	−0.2	2	1.5613×10^{-2}	1.2593×10^{-2}	1.8632×10^{-2}	−0.0468	(c)
−2	0.0	2	0.0	2	1.4443×10^{-2}	1.2600×10^{-2}	1.6287×10^{-2}	−0.0436	(b)
−2	−0.2	2	−0.2	−2	1.6554×10^{-2}	1.4540×10^{-2}	1.8569×10^{-2}	0.9859	

(a) Orthogonal signal constellation.

(b) Balanced in-phase and quadrature-phase performance, given the fact that these channels are unbalanced.

(c) Highly unbalanced in-phase and quadrature-phase performance.

Table 2 cont'd.

$\Delta\theta$, deg	Γ_1, dB	$\Delta\theta_1$, deg	Γ_2, dB	$\Delta\theta_2$, deg	$P_{b,avg}$ at $E_b/N_0 = 4$ dB	$P_{b,I}$ at $E_b/N_0 = 4$ dB	$P_{b,Q}$ at $E_b/N_0 = 4$ dB	ϕ_0, deg	Remarks
−2	−0.2	2	0.0	−2	1.5390×10^{-2}	1.4546×10^{-2}	1.6234×10^{-2}	1.0083	
−2	0.0	2	−0.2	−2	1.5568×10^{-2}	1.2560×10^{-2}	1.8576×10^{-2}	0.9797	(c)
−2	0.0	2	0.0	−2	1.4400×10^{-2}	1.2563×10^{-2}	1.6237×10^{-2}	0.9976	(a), (b)
−2	−0.2	−2	−0.2	2	1.6411×10^{-2}	1.4398×10^{-2}	1.8424×10^{-2}	0.9088	
−2	−0.2	−2	0.0	2	1.5404×10^{-2}	1.4403×10^{-2}	1.6405×10^{-2}	0.9435	
−2	0.0	−2	−0.2	2	1.5560×10^{-2}	1.2686×10^{-2}	1.8435×10^{-2}	0.8748	
−2	0.0	−2	0.0	2	1.4563×10^{-2}	1.2700×10^{-2}	1.6426×10^{-2}	0.9061	(b)
−2	−0.2	−2	−0.2	−2	1.6431×10^{-2}	1.4588×10^{-2}	1.8274×10^{-2}	1.9267	
−2	−0.2	−2	0.0	−2	1.5433×10^{-2}	1.4590×10^{-2}	1.6277×10^{-2}	1.9664	
−2	0.0	−2	−0.2	−2	1.5438×10^{-2}	1.2599×10^{-2}	1.8277×10^{-2}	1.9172	
−2	0.0	−2	0.0	−2	1.4443×10^{-2}	1.2600×10^{-2}	1.6287×10^{-2}	1.9564	(b)

(a) Orthogonal signal constellation.

(b) Balanced in-phase and quadrature-phase performance, given the fact that these channels are unbalanced.

(c) Highly unbalanced in-phase and quadrature-phase performance.

Table 3. OQPSK bit-error performance under various combinations of modulator imbalances (I/Q power ratio = 0.4 dB, E_b/N_0 = 10 dB).

$\Delta\theta$, deg	Γ_1, dB	$\Delta\theta_1$, deg	Γ_2, dB	$\Delta\theta_2$, deg	$P_{b,avg}$ at $E_b/N_0 = 10$ dB	$P_{b,I}$ at $E_b/N_0 = 10$ dB	$P_{b,Q}$ at $E_b/N_0 = 10$ dB	ϕ_0, deg	Remarks
0	0.0	0	0.0	0	6.8041×10^{-6}	3.8721×10^{-6}	9.7362×10^{-6}	0.0000	Best case
0	−0.2	2	−0.2	2	1.2708×10^{-5}	6.2368×10^{-6}	1.9178×10^{-5}	−0.9790	
0	−0.2	2	0.0	2	8.2719×10^{-6}	6.2310×10^{-6}	1.0313×10^{-5}	−0.9892	
0	0.0	2	−0.2	2	1.1686×10^{-5}	4.1013×10^{-6}	1.9270×10^{-5}	-0.9797	(c)
0	0.0	2	0.0	2	7.2252×10^{-6}	4.1119×10^{-6}	1.0339×10^{-5}	−0.9976	(a), (b)
0	−0.2	2	−0.2	−2	1.4013×10^{-5}	8.3324×10^{-6}	1.9694×10^{-5}	0.0322	
0	−0.2	2	0.0	−2	9.5274×10^{-6}	8.4295×10^{-6}	1.0625×10^{-5}	0.0336	
0	0.0	2	−0.2	−2	1.2078×10^{-5}	4.2133×10^{-6}	1.9942×10^{-5}	0.0468	(c)
0	0.0	2	0.0	−2	7.4785×10^{-6}	4.2443×10^{-6}	1.0713×10^{-5}	0.0436	(b)
0	−0.2	−2	−0.2	2	1.0950×10^{-5}	6.4124×10^{-6}	1.5488×10^{-5}	−0.0454	
0	−0.2	−2	0.0	2	8.5036×10^{-6}	6.4181×10^{-6}	1.0589×10^{-5}	−0.0337	
0	0.0	−2	−0.2	2	9.8552×10^{-6}	4.1944×10^{-6}	1.5516×10^{-5}	−0.0564	
0	0.0	−2	0.0	2	7.4516×10^{-6}	4.2254×10^{-6}	1.0678×10^{-5}	−0.0484	(b)
0	−0.2	−2	−0.2	−2	1.1570×10^{-5}	8.1292×10^{-6}	1.5012×10^{-5}	0.9755	
0	−0.2	−2	0.0	−2	9.2407×10^{-6}	8.1689×10^{-6}	1.0313×10^{-5}	0.9917	
0	0.0	−2	−0.2	−2	9.5521×10^{-6}	4.1017×10^{-6}	1.5002×10^{-5}	0.9868	
0	0.0	−2	0.0	−2	7.2252×10^{-6}	4.1119×10^{-6}	1.0339×10^{-5}	1.0024	(a), (b)

(a) Orthogonal signal constellation.

(b) Balanced in-phase and quadrature-phase performance, given the fact that these channels are unbalanced.

(c) Highly unbalanced in-phase and quadrature-phase performance.

Table 3 cont'd.

$\Delta\theta$, deg	Γ_1, dB	$\Delta\theta_1$, deg	Γ_2, dB	$\Delta\theta_2$, deg	$P_{b,avg}$ at $E_b/N_0 = 10$ dB	$P_{b,I}$ at $E_b/N_0 = 10$ dB	$P_{b,Q}$ at $E_b/N_0 = 10$ dB	ϕ_0, deg	Remarks
2	−0.2	2	−0.2	2	1.3006×10^{-5}	6.4099×10^{-6}	1.9601×10^{-5}	−1.9352	
2	−0.2	2	0.0	2	8.5036×10^{-6}	6.4181×10^{-6}	1.0589×10^{-5}	−1.9663	
2	0.0	2	−0.2	2	1.2040×10^{-5}	4.2169×10^{-6}	1.9863×10^{-5}	−1.9125	(c)
2	0.0	2	0.0	2	7.4516×10^{-6}	4.2254×10^{-6}	1.0678×10^{-5}	−1.9516	(b)
2	−0.2	2	−0.2	−2	1.5205×10^{-5}	8.9850×10^{-6}	2.1426×10^{-5}	−0.9219	
2	−0.2	2	0.0	−2	1.0408×10^{-5}	9.1824×10^{-6}	1.1633×10^{-5}	−0.9412	
2	0.0	2	−0.2	−2	1.3260×10^{-5}	4.5646×10^{-6}	2.1955×10^{-5}	−0.8868	(c)
2	0.0	2	0.0	−2	8.2417×10^{-6}	4.6377×10^{-6}	1.1846×10^{-5}	−0.9109	
2	−0.2	−2	−0.2	2	1.0624×10^{-5}	6.2366×10^{-6}	1.5012×10^{-5}	−0.9992	
2	−0.2	−2	0.0	2	8.2719×10^{-6}	6.2310×10^{-6}	1.0313×10^{-5}	−1.0108	
2	0.0	−2	−0.2	2	9.5520×10^{-6}	4.1017×10^{-6}	1.5002×10^{-5}	−0.9868	
2	0.0	−2	0.0	2	7.2252×10^{-6}	4.1119×10^{-6}	1.0339×10^{-5}	−1.0024	(a), (b)
2	−0.2	−2	−0.2	−2	1.1881×10^{-5}	8.2729×10^{-6}	1.5489×10^{-5}	0.0240	
2	−0.2	−2	0.0	−2	9.5160×10^{-6}	8.3724×10^{-6}	1.0660×10^{-5}	0.0169	
2	0.0	−2	−0.2	−2	9.8552×10^{-6}	4.1944×10^{-6}	1.5516×10^{-5}	0.0564	
2	0.0	−2	0.0	−2	7.4516×10^{-6}	4.2254×10^{-6}	1.0678×10^{-5}	0.0484	(b)
−2	−0.2	2	−0.2	2	1.3166×10^{-5}	6.4104×10^{-6}	1.9922×10^{-5}	−0.0228	
−2	−0.2	2	0.0	2	8.5566×10^{-6}	6.4175×10^{-6}	1.0696×10^{-5}	−0.0120	
−2	0.0	2	−0.2	2	1.2078×10^{-5}	4.2133×10^{-6}	1.9942×10^{-5}	−0.0468	(c)
−2	0.0	2	0.0	2	7.4785×10^{-6}	4.2443×10^{-6}	1.0713×10^{-5}	−0.0436	(b)
−2	−0.2	2	−0.2	−2	1.3655×10^{-5}	8.1284×10^{-6}	1.9182×10^{-5}	0.9859	
−2	−0.2	2	0.0	−2	9.2407×10^{-6}	8.1689×10^{-6}	1.0313×10^{-5}	1.0083	
−2	0.0	2	−0.2	−2	1.1686×10^{-5}	4.1013×10^{-6}	1.9270×10^{-5}	0.9797	(c)
−2	0.0	2	0.0	−2	7.2252×10^{-6}	4.1119×10^{-6}	1.0339×10^{-5}	0.9976	(a), (b)
−2	−0.2	−2	−0.2	2	1.1967×10^{-5}	6.9533×10^{-6}	1.6981×10^{-5}	0.9088	
−2	−0.2	−2	0.0	2	9.2765×10^{-6}	6.9994×10^{-6}	1.1554×10^{-5}	0.9435	
−2	0.0	−2	−0.2	2	1.0827×10^{-5}	4.5240×10^{-6}	1.7129×10^{-5}	0.8748	
−2	0.0	−2	0.0	2	8.1833×10^{-6}	4.5972×10^{-6}	1.1770×10^{-5}	0.9061	
−2	−0.2	−2	−0.2	−2	1.1956×10^{-5}	8.4140×10^{-6}	1.5499×10^{-5}	1.9267	
−2	−0.2	−2	0.0	−2	9.5274×10^{-6}	8.4295×10^{-6}	1.0625×10^{-5}	1.9664	
−2	0.0	−2	−0.2	−2	9.8830×10^{-6}	4.2364×10^{-6}	1.5530×10^{-5}	1.9172	
−2	0.0	−2	0.0	−2	7.4785×10^{-6}	4.2443×10^{-6}	1.0713×10^{-5}	1.9564	(b)

(a) Orthogonal signal constellation.

(b) Balanced in-phase and quadrature-phase performance, given the fact that these channels are unbalanced.

(c) Highly unbalanced in-phase and quadrature-phase performance.

Another interesting conclusion is that the worst combination of modulator imbalances tends to happen when the amplitude imbalance is at its maximum and the phase imbalance for the in-phase and quadrature-phase channels makes them rotate towards each other on a signal phasor plane, which agrees well with one's intuition. The best and the worst combinations for these bit-error probabilities as functions of E_b/N_0 are plotted in Figs. 4 through 6 for the case of perfect carrier synchronization, and in Figs. 7 through 9 for the case of imperfect carrier synchronization with a finite loop SNR of 22 dB. Simulation points, which agree with the analytical results, also are included in Figs. 7 through 9.

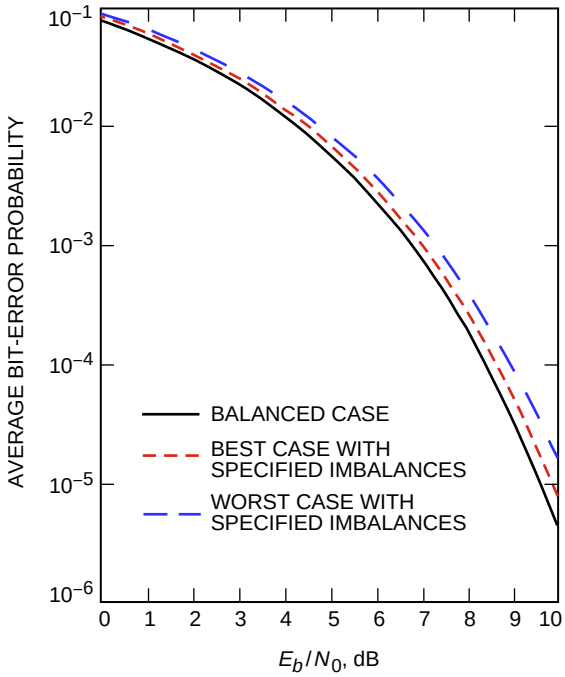

Fig. 4. Bit-error performance of OQPSK signals under perfect carrier synchronization.

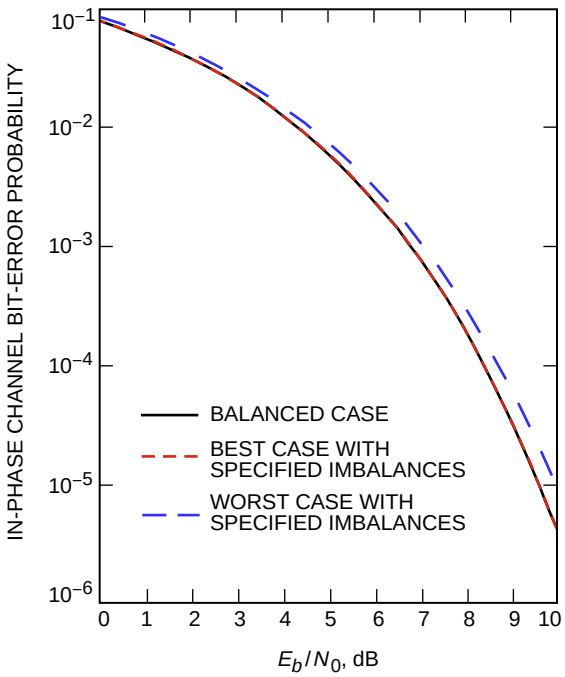

Fig. 5. Bit-error performance of OQPSK signals under perfect carrier synchronization: in-phase channel.

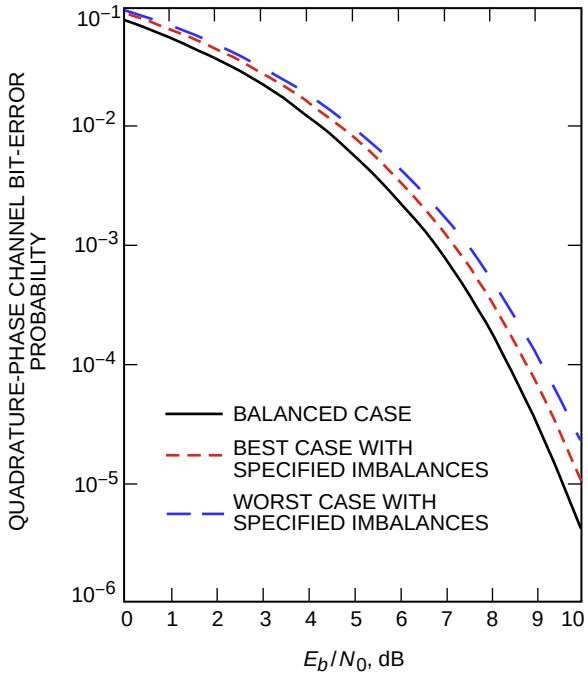

Fig. 6. Bit-error performance of OQPSK signals under perfect carrier synchronization: quadrature-phase channel.

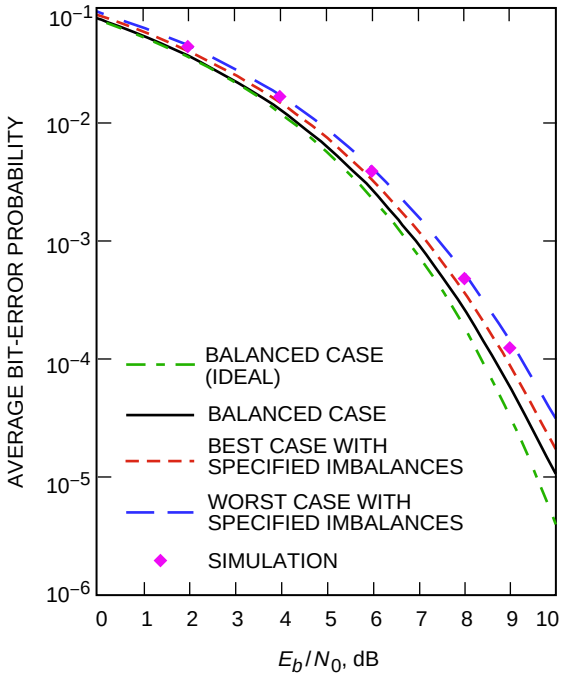

Fig. 7. Bit-error performance of OQPSK signals under imperfect carrier synchronization.

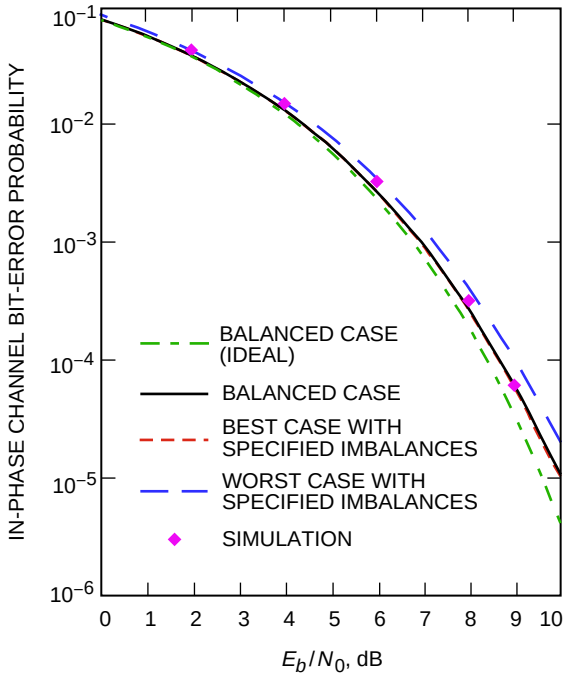

Fig. 8. Bit-error performance of OQPSK signals under imperfect carrier synchronization: in-phase channel.

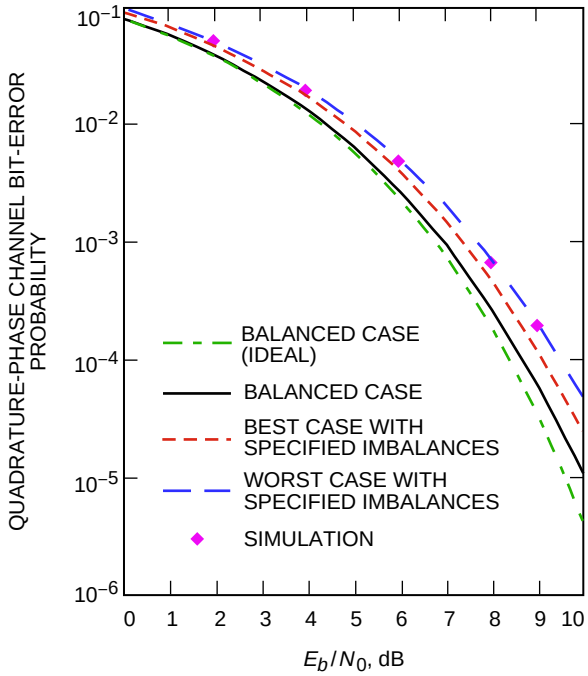

Fig. 9. Bit-error performance of OQPSK signals under imperfect carrier synchronization: quadrature-phase channel.

From Figs. 4 through 6, a 0.34-dB I-channel and a 0.75-dB Q-channel worst-case E_b/N_0 degradation at the bit-error probability of 10^{-4} are shown under the assumption of perfect carrier synchronization for the CCSDS recommendation of a 2-deg maximum permissible phase imbalance and a 0.2-dB amplitude imbalance. The inferior performance in the Q-channel is expected because of its 0.4-dB power deficiency as a result of the interchannel amplitude imbalance. The overall degradation for averaged performance is 0.58 dB. The actual performance becomes worse when imperfect carrier tracking is considered. For example, for a carrier tracking loop operated at a 22-dB loop SNR, Figs. 7 through 9 show a 0.61-dB I-channel and a 1.08-dB Q-channel worst-case degradation at the same bit-error probability, and the overall degradation for averaged performance becomes 0.86 dB when compared with the perfect carrier synchronization case.

VI. Conclusion

In this article, the effects of modulator imbalances on the carrier-suppression level and the bit-error performance for an OQPSK system are analyzed. Numerical results and performance comparisons are given for the CCSDS recommended maximum permissible amplitude and phase imbalances. The carrier-suppression level and worst-case bit-error probability figures obtained from this analysis suggest that the current CCSDS recommendation of a maximum permissible phase imbalance of 2 deg and amplitude imbalance of 0.2 dB would be sufficient for a carrier-suppression level of 25 dB or more and a system degradation of 1 dB or less at the bit-error probability of 10^{-4} for an OQPSK system operated in a reasonable loop SNR region.

References

[1] B. A. Carlson, *Communication Systems*, 2nd edition, New York: McGraw-Hill, 1975.

[2] H. Tsou, "The Effect of Phase and Amplitude Imbalance on the Performance of BPSK/QPSK Communication Systems," *The Telecommunications and Data Acquisition Progress Report 42-130, April–June 1997*, Jet Propulsion Laboratory, Pasadena, California, pp. 1–13, August 15, 1997.
http://tmo.jpl.nasa.gov/tmo/progress_report/42-130/130B.pdf

[3] Consultative Committee for Space Data Systems, *Recommendations for Space Data System Standards: Radio Frequency and Modulation Systems, Part 1, Earth Stations and Spacecraft*, CCSDS 401.0-B, Blue Book, November 1994.

[4] M. K. Simon, "Carrier Synchronization of Offset Quadrature Phase-Shift Keying," *The Telecommunications and Mission Operations Progress Report 42-133, January–March 1998*, Jet Propulsion Laboratory, Pasadena, California, pp. 1–33, May 15, 1998.
http://tmo.jpl.nasa.gov/tmo/progress_report/42-133/133J.pdf